Generation of an isolated few-attosecond pulse in optimized inhomogeneous two-color fields

Yi Chou, Peng-Cheng Li, Tak-San Ho, and Shih-I Chu

Phys. Rev. A **92**, 023423 — Published 28 August 2015

DOI: 10.1103/PhysRevA.92.023423

Generation of an isolated few-attosecond pulse in optimized inhomogeneous two-color fields

Yi Chou[1,*] Peng-Cheng Li[1,2,†] Tak-San Ho[3,‡] and Shih-I Chu[1,4,§]
[1] *Center for Quantum Science and Engineering, Department of Physics, and Center for Advanced Study in Theoretical Sciences, National Taiwan University, Taipei 10617, Taiwan*
[2] *College of Physics and Electronic Engineering, Northwest Normal University, Lanzhou 730070, China*
[3] *Department of Chemistry, Princeton University, Princeton, N.J. 08544, USA*
[4] *Department of Chemistry, University of Kansas, Kansas 66045, USA*

We present a numerical study for optimization of ultrabroad supercontinuum spectrum by controlling the waveforms of laser fields, with an ultimate goal to generate isolated ultrashort attosecond pulses. Specifically, we extend a derivative-free nonconvex optimization algorithm for maximization of the supercontinnum power spectrum near the HHG cutoff. It is found that optimally shaped inhomogeneous two-color midinfrared laser fields can greatly enhance and extend high-order harmonic generation plateau. Wavelet time-frequency analysis and classical simulations show that the superposition of resulting hydrogen HHG supercontinuum effectively gives rise to a robust isolated 5-attosecond pulse.

PACS numbers: 32.70.Jz,42.50.Hz,32.80.Qk

I. INTRODUCTION

The advance of attosecond (as) pulse technology has attracted immense interest over the past decades, since it enables observation and control of the dynamic process of electrons in atoms, molecules and solids in the nature time scale[1–3]. The coherent superposition of a broadband supercontinuum in high-order harmonic generation (HHG) is the most reliable way to generate ultrashort pulses [3–5]. The HHG spectrum is characterized by a dramatic drop at low orders followed by a typically broad plateau where all the harmonics have a similar strength, and terminated with a sharp cutoff at the end of plateau, beyond which no further harmonic emission occurs. Typically, for atomic gases the maximum cutoff of the HHG energy is given approximated by the formula $I_p+3.17U_p$, where I_p is the atomic ionization potential and U_p is the ponderomotive potential. The physical features of the HHG can be qualitatively understood by a semiclassical three-step model [6, 7]. According to the three-step model, the electron is first ionized toward continuum by tunnelling through the field-modified potential barrier, then accelerated in the laser field, and finally driven back to recollide with the parent ion and emit high-energy photons.

In a recent experiment, Chang *et al* [8] have successfully produced a 67-attosecond pulse, which is the shortest attosecond pulse known at present. In theoretical studies, many optimization schemes of controlling laser pulses to generate attosecond pulses have been proposed using, for examples, chirp lasers [9], two-color fields [9–12], and three-color fields [13, 14]. Numerical simulations showed that the optimized laser pulses could significantly extend the HHG cutoff and the supercontinuum near the cutoff. However, in general, superposing the harmonics in extended supercontinuum cutoff regime may fail to generate a shorter attosecond pulse [10, 15] due to possibility of concurrent happening of both the long and short quantum paths in that regime. It is well known that generation of isolated attosecond pulses is a manifestation of phase matching of just one-type of (i.e. either long or short, but not both) quantum paths in the supercontinuum regime [16, 17]. Simultaneous superposition of both long and short quantum paths can destructively interfere with each other

In a different experiment, Kim *et al* [18] have shown that spatially inhomogeneous laser fields could enhance the surface plasmon resonance HHG. In their study, the output laser was amplified by a factor of 20-40 dB compared to the incident laser field. Moreover, the effect of the resonant plasmons within a metallic nanostructure in the presence of a spatially linearly varying inhomogeneous field has been theoretical studied using the first-order approximation with respect to position [19, 20]. In particular, several theoretical studies have demonstrated that using spatially inhomogeneous fields could not only considerably broaden the HHG of the plateau region but also effectively select an single quantum path in the supercontinuum regime [21–24].

The optimal control theory (OCT) [25, 26] is a powerful tool to find optimized external fields that steers the system to a certain objective with the maximum yield. It has been widely applied to controlling various atomic and molecular processes [27], including enhancing and suppressing the ionization [28, 29].

In this paper, we present numerical simulations to study the HHG processes of a hydrogen atom using op-

* r00222008@ntu.edu.tw
† lipc@nwnu.edu.cn
‡ tsho@princeton.edu
§ sichu@ku.edu

timized inhomogeneous two-color midinfrared (IR) laser pulses, aiming to enhance the HHG plateau and extend the HHG cutoff, and ultimately to generate an isolated ultrashort attosecond laser pulse via superposing ultrabroad HHG supercontinuum. For exploring the HHG power spectra, the time-dependent Schrödinger equation (TDSE) is solved numerically accurately and efficiently with the time-dependent generalized pseudospectral method (TDGPS) [30]. To understand the contributions of quantum trajectories, we also perform the wavelet time-frequency analysis of HHG as well as classical simulation, see Sec. III. Our simulations show in Sec. IV that an ultrabroadband supercontinuum can produce a 5-as pulse with an optimized inhomogeneous two-color mid-IR laser pulse. Finally, we draw a short summary of this work in Sec. V.

II. THEORETICAL FORMULATION

To investigate the quantum dynamics in strong laser fields, we numerically solve the TDSE (in atomic units)

$$i\frac{\partial\psi(\mathbf{r},t)}{\partial t} = \hat{H}(\mathbf{r},t)\psi(\mathbf{r},t) = \left[\hat{H}_0(\mathbf{r}) + \hat{V}(\mathbf{r},t)\right]\psi(\mathbf{r},t), \tag{1}$$

where $\hat{H}_0(\mathbf{r})$ and $\hat{V}(\mathbf{r},t)$, respectively represents the unperturbed Hamiltonian and the coupling between the atom and the laser field. In this study, $\hat{H}_0(\mathbf{r})$ is written as

$$\hat{H}_0(\mathbf{r}) = -\frac{1}{2}\nabla^2 - \frac{1}{r}, \tag{2}$$

and $\hat{V}(\mathbf{r},t)$ as

$$\hat{V}(\mathbf{r},t) = -\mathbf{E}(\mathbf{r},t)\cdot\mathbf{r} = -E(t)\left(1+\beta z\right)z, \tag{3}$$

for a hydrogen atom and a spatially inhomogeneous and linearly polarized laser field $\mathbf{E}(\mathbf{r},t)$ along the z axis, where $E(t)$ is the temporal component laser field and β (in the reciprocal length) denotes the inhomogeneity of the laser field. The linear spatial approximation $(1+\beta z)\,z$ of inhomogeneous laser field has been extensively used in previous investigations on plasmon-driven HHG [21–24].

We solve the TDSE, Eq.(1), using the TDGPS method [30] in the spherical coordinates. Specifically, the TDGPS is implemented as follows. First, we use a nonuniformly discretized spatial grid generated by the generalized pseudospectral method for optimum representation of the wave function. Then, we invoke the second-order split-operator (SO) technique in the energy representation for efficient and accurate time propagation of the underlying time-dependent wave function. The second-order SO method can be written as

$$\begin{aligned}\psi(\mathbf{r},t+\Delta t) \simeq & \exp\left(-i\hat{H}_0\frac{\Delta t}{2}\right) \\ & \times \exp\left[-i\hat{V}\left(\mathbf{r},\theta,t+\frac{\Delta t}{2}\right)\Delta t\right] \\ & \times \exp\left(-i\hat{H}_0\frac{\Delta t}{2}\right)\psi(\mathbf{r},t) + O(\Delta t^3),\end{aligned} \tag{4}$$

where Δt is a sufficiently small time step for the propagation.

Once the corresponding time-dependent wave function is obtained via Eq.(4), the expectation value of the induced dipole acceleration can be evaluated using the expression

$$d_A(t) = \frac{\partial^2}{\partial t^2}\left\langle\psi(\mathbf{r},t)\right| z \left|\psi(\mathbf{r},t)\right\rangle, \tag{5}$$

where the two-color mid-IR laser is composed of two pulses as follows:

$$\begin{aligned}E(t) = & A_1 f_1(t)\cos(\omega_1 t+\phi_1) \\ & + A_2 f_2(t)\cos(\omega_2 t+\phi_2),\end{aligned} \tag{6}$$

with $A_{i=1,2}$, $f_i(t)$, ω_i and ϕ_i denoting, respectively, the electric-field amplitude, the Gaussian envelope, the frequencies and the carrier-envelope phases (CEP) of the two pulses. From Eq.(5) we can compute the HHG power spectra by Fourier transforming the time-dependent dipole acceleration d_A, i.e.

$$P_A(\omega) = \left|\frac{1}{t_f-t_i}\frac{1}{\omega^2}\int_{ti}^{t_f} d_A(t)e^{-i\omega t}dt\right|^2. \tag{7}$$

Moreover, a detailed time-frequency analysis of HHG spectrum can be made via the wavelet transform of the induced dipole acceleration $d_A(t)$ using the relation [31]

$$A(t,\omega) = \int d_A(t')\sqrt{\omega}W(\omega(t'-t))dt', \tag{8}$$

where the Morlet mother wavelet $W(t'-t)$ is given as

$$W(x) = \frac{1}{\sqrt{\tau_0}}e^{ix}e^{\frac{-x^2}{2\tau_0^2}}. \tag{9}$$

Finally, an attosecond pulse can be realized by superposing the supercontinuum harmonics over a finite frequency window $[\omega_i,\omega_f]$, and its temporal intensity can be computed via the relation

$$I(t) = \left|\int_{\omega_i}^{\omega_f} D_A(\omega)e^{i\omega t}d\omega\right|, \tag{10}$$

where $D_A(\omega) = \int d_A e^{-i\omega t}dt$ and ω_i and ω_f are determined judiciously for generating the shortest attosecond pulse.

III. OPTIMIZATION OF CONTROL LASER FIELDS

In the numerical OCT simulations below, only a subset of parameters of the two-color laser control field, Eq.(6), were optimized iteratively. These parameters include the CEPs ϕ_1, ϕ_2 and the amplitude sum $A = A_1 + A_2$ (the ratio A_1/A_2, the frequencies ω_1 and ω_2, and the Gaussian functions $f_{1,2}(t)$ are kept fixed throughout). The inclusion of A as an optimal control parameter permits the extension of the cutoff without compromising on the efficiency in the generation of HHG plateau. Specifically, the optimization is performed by maximizing the merit function

$$J\left[\phi_1, \phi_2, A\right] = \int_{\omega_L}^{\omega_H} \log_{10} P_A(\omega) d\omega, \tag{11}$$

where ω_L and ω_H are, respectively, the lowest and highest frequencies of the frequency window to be integrated over the HHG power spectra (in log-scale) for generating the coveted ultrashort attosecond pulse. In the following calculations, to enhance and extend the HHG near the cutoff, we have chosen a proper frequency window $[\omega_L, \omega_H]$ between 500th and 1600th harmonic orders. We achieve the maximization of the merit function, i.e.,

$$\max_x J\left[x\right], \; x = \{\phi_1, \phi_2, A\} \tag{12}$$

via NEWUOA software [32], which is a recently developed derivative-free nonconvex optimization algorithm.

IV. RESULT AND DISCUSSION

All of results presented in this section correspond to Gaussian envelope functions $f_1(t), f_2(t)$ with a FWHM equal to 8 fs and an inhomogeneous parameter $\beta = 0.003$ for the inhomogeneous two-color laser fields. Fig. 1(a) depicts the initial right-shifted laser pulse (blue line) [with $\omega_1 = 0.0228$ a.u. (2000 nm), $A_1 = 0.0577$ *a.u.* and $\phi_1 = 0$, $\omega_2 = 0.043$ a.u. (1064 nm), $A_2 = 0.0258$ *a.u.* and $\phi_2 = -0.75\pi$] and the optimized pulse (red line) [with $\phi_1 = 0.334\pi$, $\phi_2 = -0.73\pi$, $A_1 = 0.0635$ a.u. (1.4×10^{14} W/cm^2) and $A_2 = 0.0284$ a.u. (2.8×10^{13} W/cm^2)] which resembles a left-shifted pulse as a consequence of spatial inhomogeneity inherent in the control pulse. In this regard, it has been shown that a right-shifted laser pulse, whose peak amplitude arrives after one half of laser-operation time, is more likely to bring about a broad HHG plateau of HHG [12].

Fig. 1(b) shows the HHG spectra for the inhomogeneous initial field (blue curve) and optimized field (red curve). For comparison, we also plot the HHG spectrum for a homogeneous initial pulse field ($\beta = 0$) (green line). It was found that the inhomogeneous fields can not only substantially extend the HHG cutoff but also generate an ultrabroad supercontinuum, while the homogeneous field can only produce a narrow band of continuous harmonics near the cutoff. In particular, the optimized HHG plateau is greatly heightened and extended over its non-optimized counterpart. The optimized supercontinuum is also significantly broadened and the location of cutoff is shifted from the 950th order to the 1400th order as a result of optimization. Here we noted that the HHG energy cut-off for the homogeneous pulse (green curve in Fig 1(b)) is around 300th order, which is substantially less than those for both initial and optimized inhomogeneous pulses(blue and red curves). The results in

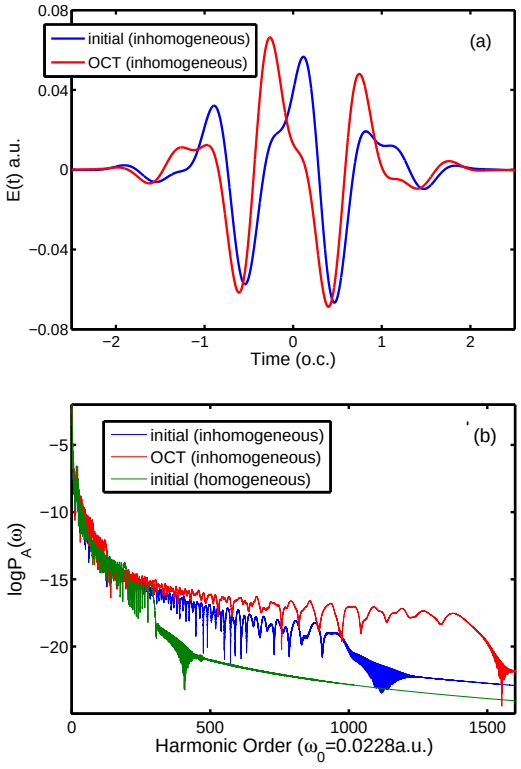

FIG. 1. (color online) (a) The initial laser field (blue line) : $\omega_1 = 0.0228$ a.u. (2000 nm), $A_1 = 0.0577$ *a.u.* and $\phi_1 = 0$, $\omega_2 = 0.043$ a.u. (1064 nm), $A_2 = 0.0258$ *a.u.* and $\phi_2 = -0.75\pi$, and the optimized laser field (red line) : $\phi_1 = 0.334\pi$, $\phi_2 = -0.73\pi$, $A_1 = 0.0635$ a.u. (1.4×10^{14} W/cm^2) and $A_2 = 0.0284$ a.u. (2.8×10^{13} W/cm^2). (b) The HHG spectra for each case.

Fig. 1(a) and 1(b) show that the optimization of the laser CEPs are mainly responsible for the drastic enhancement and extension of the HHG plateau and cut-off energy, to be understood as follows. Since it is well known that the ponderomotive potential $U_p \propto I\lambda^2$ as a function of laser intensity I and wavelength λ, an increase of the laser amplitude generally extends the HHG cutoff energy [33]. However, it is unlikely to increase the laser intensity indefinitely due to the limitation in ionization potential as well as the saturation effect of the ionization. Fig. 1(a) clearly shows that the amplitude of the optimized pulse is merely 1.18 times larger than the initial one, indicating

that the observed large improvement of the HHG generation is mainly a result of the optimized CEP. Clearly, the optimization of the intensities and CEP phases, resulting in reacceleration of the electron before returning to the ion, gives rise to high HHG yields between orders 500 and 1400. Moreover, away from the origin of hydrogen atom, the ionized electron undergoes a faster and faster acceleration due to a gradually increased intensity of inhomogeneous laser fields. As a result of the increasing acceleration away from the center of hydrogen atom and the saturation effect of the electron ionization, a right-shifted spatially inhomogeneous pulse is no longer suitable for broadening the underlying HHG plateau, as shown in Fig. 1(a) and 1(b), contrary to the case of spatially homogeneous pulse.

To further understand the extension of HHG plateau cutoff, we also perform additional classical simulations and quantum wavelet time-frequency analysis. The former were carried out by solving the classical Newton equation for electron motion in the laser fields, here $\ddot{z}(t) = -\nabla_z \hat{V}(z,t) = (1 + 2\beta z(t))E(t)$, while the latter was performed using Eq.(8). The classical returning energy maps (yellow lines) in Fig. 2 clearly show that the maximum kinetic energy of the returning electron is in good agreement with the cutoffs of the HHG spectra in Fig. 1(b).

Fig. 2 also shows the results of the wavelet time-frequency analysis. It was found that with the homogeneous field, due to the wide extent of their emission times, Fig. 2(a) it is ineffective unlikely to superpose the plateau harmonics from 260th to 310th order for producing an ultrashort attosecond pulse. In contrast, with both the initial and optimized inhomogeneous pulses, due to their much shorter emission time span, Fig. 2(b) and 2(c), it is straightforward to superpose the corresponding supercontinuum harmonics near the cutoff. Moreover, as seen in Fig. 2(b) and 2(c), the sub-peaks of HHG emission in the inhomogeneous fields are drastically suppressed, because parts of ionized electrons fail to return to the parent ion [34]. In the optimized inhomogeneous pulse the returning electrons favor long trajectories, all come back to the atom simultaneously and are responsible for the HHG generation from about between 500th and 1600th order. Similarly, in the initial inhomogeneous pulse the long-trajectory electrons also dominate the harmonics, here from 600th order to 900th. Importantly, the optimization of the inhomogeneous pulse also greatly reduces the contribution of the short-trajectory electron emission. These observations provide the physical underpinning for further cutting down the length of isolated ultrashort attosecond pulses with either long or short returning quantum trajectory path, but not both. We further remark that the total intensity of each harmonic order (as shown in Fig. 1) is related to the time integral in the time-frequency profile (Fig. 2). For the homogeneous case, the distribution of harmonics between 200 and 300 is broad in time, but the corresponding magnitude is smaller, as shown on the right panel in Fig. 2(a). Therefore, the intensities of the harmonic orders between 200 and 300 are similar for all three cases, as shown in Fig. 1.

Fig. 3 depicts intensities of attosecond pulses generated in the inhomogeneous initial and optimized fields: (a) an isolated 19-as pulse from superposing the harmonics from the 600th to the 900th order generated by the initial laser pulse, and (b) a much shorter single 5-as pulse from superposing all harmonics between the 486th and the 1596th order generated by the optimized laser pulse. Remarkably, the optimized attosecond pulse is enhanced by a hundredfold over the unoptimized one. Especially, it is important to note that all of the ultrabroad supercontinuum harmonics of the optimized two-color inhomogeneous fields were nearly coherently superposed, making possible very efficient generation of a greatly enhanced and ultrashort attosecond pulse as seen in Fig. 3(b). Fig. 4 shows the time profile of a series of harmonics constituting the 5-as pulse, in which each harmonic is synchronized with each other, for generating a robust attosecond pulse. We note that, the HHG generation has a close relation to the single-atom response as well as macroscopic phase matching. For the macroscopic propagation of supercontinuum harmonics, it has been found that, while the HHG emission with short quantum path is increased, the HHG emission with long quantum path would not change after the macroscopic propagation [35]. As a result, the single attosecond pulse generating by inhomogeneous fields can be produced by spatial filtering.

V. CONCLUSION

In conclusion, we have demonstrated that it is possible to optimize spatially inhomogeneous two-color mid-IR laser fields for generating single ultrashort attosecond pulse in atomic hydrogen. Even though there have been several studies using inhomogeneous one- or two-color fields for generating isolated attosecond pulses [21–24], optimal control of inhomogeneous fields has never been performed in those studies. The current study is the first to demonstrate the possibility of generating an isolated ultrashort few-attosecond pulse via careful optimization of the spatially inhomogeneous two-color fields. By optimizing both the field intensity and CEPs, the resultant inhomogeneous laser pulse not only enhances the HHG plateau, but also extends its cutoff greatly. As a result, a robust isolated 5-as pulse can be produced by superposing the corresponding ultrabroad supercontinuum. The magnitude of the optimized attosecond pulse is two orders of magnitude over its unoptimized counterpart as a result of using the entire supercontinuum region effectively. The inhomogeneous laser fields considered in the present study should be achievable in laboratories, thus, making possible the realization of ultrashort few-attosecond pulses experimentally.

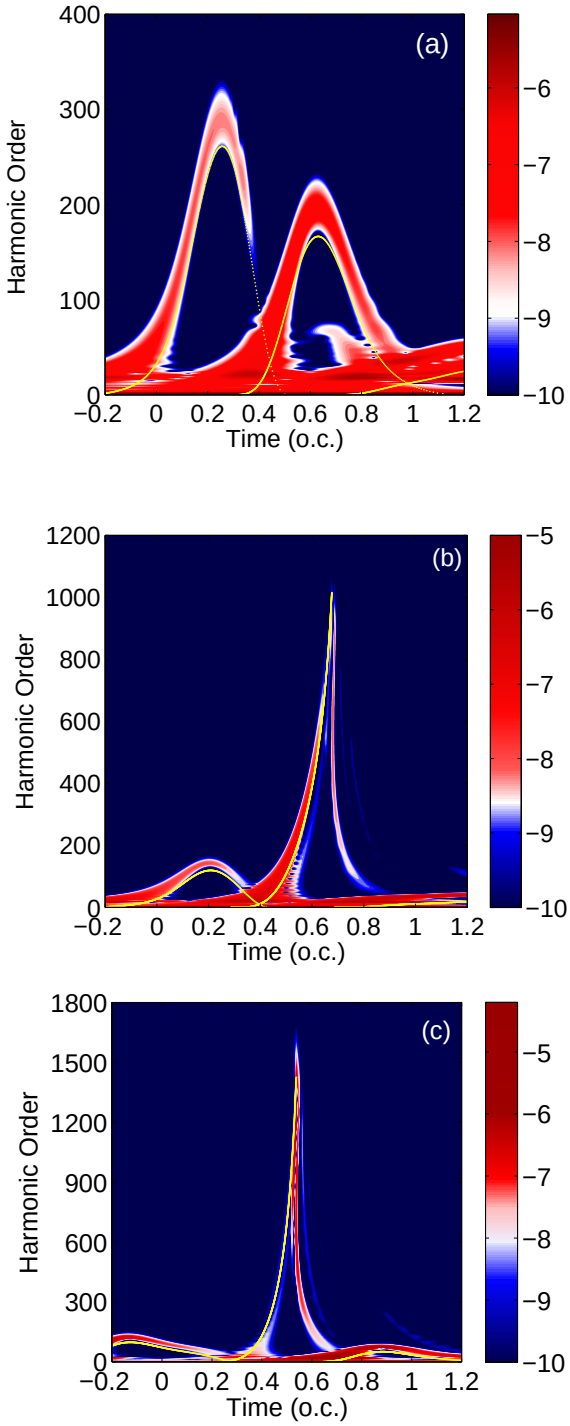

FIG. 2. (color online) Wavelet time-frequency profiles of the HHG spectra and classical returning energy maps (yellow solid-lines) of hydrogen atoms driven by the initial homogeneous field (a), the initial inhomogeneous field (b) and optimized inhomogeneous field (c).

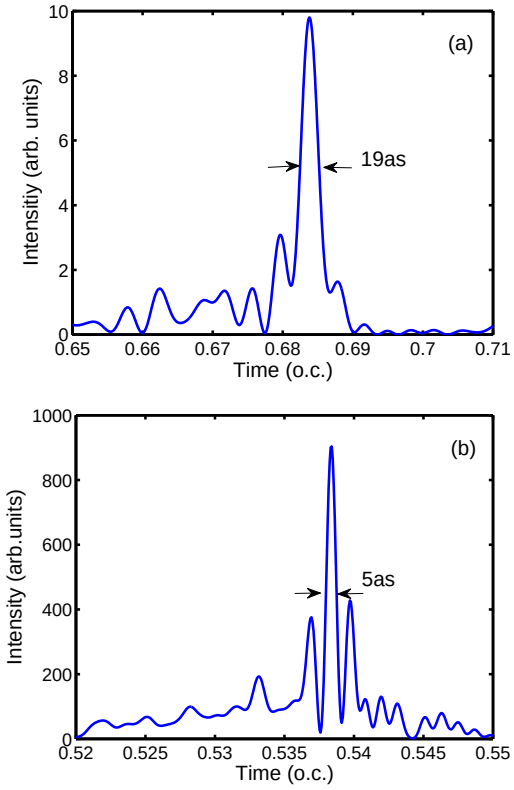

FIG. 3. (color online) Attosecond pulses by synthesizing the harmonic order of: (a) 600th-900th for inhomogeneous initial laser field. (b) 486th-1596th for inhomogeneous optimized laser field.

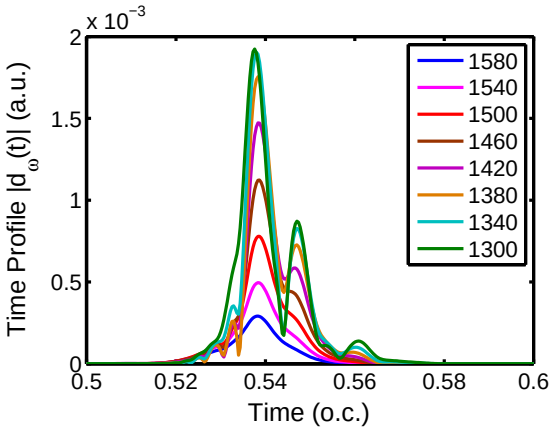

FIG. 4. (color online) The corresponding time profile of the consecutive harmonics in generation of the 5-as pulse.

VI. ACKNOWLEDGMENTS

This work was partially supported by the Chemical Sciences, Geosciences, and Biosciences Division of the Office of Basic Energy Sciences, Office of Sciences, US Department of Energy and by the US National Science

Foundation. We also would like to thank the partial support of the Ministry of Science and Technology of Taiwan and National Taiwan University (Grants No.104R8914 and No. 104R8700-2). P.-C.L. is partially supported by National Natural Science Foundation of China (Grants No. 11364039 and No. 11465016), Natural Science Foundation of Gansu Province (Grant No. 1308RJZA195), and Education Department of Gansu Province (Grant No. 2014A-010).

[1] F. Krausz and M. Ivanov, Rev. Mod. Phys. **81**, 163 (2009).
[2] Z. Chang and P. Corkum, J. Opt. Soc. Am. B **27**, B9 (2010).
[3] E. Goulielmakis, M. Schultze, M. Hofstetter, V. S. Yakovlev, J. Gagnon, M. Uiberacker, A. L. Aquila, E. M. Gullikson, D. T. Attwood, R. Kienberger, F. Krausz, and U. Kleineberg, Science **320**, 1614 (2008).
[4] G. Sansone, E. Benedetti, F. Calegari, C. Vozzi, L. Avaldi, R. Flammini, L. Poletto, P. Villoresi, C. Altucci, R. Velotta, S. Stagira, S. De Silvestri, and M. Nisoli, Science **314**, 443 (2006).
[5] J. J. Carrera, X. M. Tong, and S. I. Chu, Phys. Rev. A **74**, 023404 (2006).
[6] P. B. Corkum, Phys. Rev. Lett. **71**, 1994 (1993).
[7] K. C. Kulander, K. J. Schafer, and J. L. Krause, in *Super Intense Laser-Atom Physics*, Vol. 316 of NATO Advanced Study Institute, Series B: Physics, edited by B. Piraux, A. L'Huillier, and Rzażewski (Plenum, New York, 1993) p. 95.
[8] K. Zhao, Q. Zhang, M. Chini, Y. Wu, X. Wang, and Z. Chang, Opt. Lett. **37**, 3891 (2012).
[9] J. Xu, B. Zeng, and Y. Yu, Phys. Rev. A **82**, 053822 (2010).
[10] L. Feng and T. Chu, Phys. Rev. A **84**, 053853 (2011).
[11] P.-C. Li, C. Laughlin, and S.-I. Chu, Phys. Rev. A **89**, 023431 (2014).
[12] I.-L. Liu, P.-C. Li, and S.-I. Chu, Phys. Rev. A **84**, 033414 (2011).
[13] L. Feng and T. Chu, Physics Letters A **375**, 3641 (2011).
[14] P.-C. Li, I.-L. Liu, and S.-I. Chu, Opt. Express **19**, 23857 (2011).
[15] L.-Q. Feng, Y.-B. Duan, and T.-S. Chu, Annalen der Physik **525**, 915 (2013).
[16] J.-G. Chen, Y.-J. Yang, S.-L. Zeng, and H.-Q. Liang, Phys. Rev. A **83**, 023401 (2011).
[17] C.-L. Xia and X.-S. Liu, Phys. Rev. A **87**, 043406 (2013).
[18] S. Kim, J. Jin, Y.-J. Kim, I.-Y. Park, Y. Kim, and S.-W. Kim, Nature **453**, 757 (2008).
[19] T. Shaaran, M. F. Ciappina, and M. Lewenstein, Phys. Rev. A **86**, 023408 (2012).
[20] S. H. Hekmatara, M. Mohebbi, and J. Rahpeyma, RSC Adv. **4**, 59064 (2014).
[21] M. F. Ciappina, J. Biegert, R. Quidant, and M. Lewenstein, Phys. Rev. A **85**, 033828 (2012).
[22] J. A. Pérez-Hernández, M. F. Ciappina, M. Lewenstein, L. Roso, and A. Zaír, Phys. Rev. Lett. **110**, 053001 (2013).
[23] I. Yavuz, E. A. Bleda, Z. Altun, and T. Topcu, Phys. Rev. A **85**, 013416 (2012).
[24] X. Cao, S. Jiang, C. Yu, Y. Wang, L. Bai, and R. Lu, Opt. Express **22**, 26153 (2014).
[25] C. Brif, R. Chakrabarti, and H. Rabitz, New Journal of Physics **12**, 075008 (2010).
[26] J. Werschnik and E. K. U. Gross, Journal of Physics B: Atomic, Molecular and Optical Physics **40**, R175 (2007).
[27] K. Krieger, A. Castro, and E. Gross, Chemical Physics **391**, 50 (2011).
[28] A. Castro, E. Rsnen, A. Rubio, and E. K. U. Gross, EPL (Europhysics Letters) **87**, 53001 (2009).
[29] M. Hellgren, E. Räsänen, and E. K. U. Gross, Phys. Rev. A **88**, 013414 (2013).
[30] X.-M. Tong and S.-I. Chu, Chemical Physics **217**, 119 (1997), dynamics of Driven Quantum Systems.
[31] X.-M. Tong and S.-I. Chu, Phys. Rev. A **61**, 021802 (2000).
[32] M. Powell, in *Large-Scale Nonlinear Optimization*, Nonconvex Optimization and Its Applications, Vol. 83, edited by G. Di Pillo and M. Roma (Springer US, 2006) pp. 255–297.
[33] J. L. Krause, K. J. Schafer, and K. C. Kulander, Phys. Rev. Lett. **68**, 3535 (1992).
[34] C. Yu, Y. Wang, X. Cao, S. Jiang, and R. Lu, Journal of Physics B: Atomic, Molecular and Optical Physics **47**, 225602 (2014).
[35] P.-C. Li, C. Laughlin, and S. I. Chu, Phys. Rev. A **89**, 023431 (2014).